Journal of Polymer Research (2020) 27: 183
https://doi.org/10.1007/s10965-020-02158-6

ORIGINAL PAPER

Development of dopamine biosensor based on polyaniline/carbon quantum dots composite

Chanida Ratlam [1,2] · Sukon Phanichphant [3] · Saengrawee Sriwichai [1,3]

Received: 9 January 2020 / Accepted: 8 May 2020 / Published online: 30 June 2020

Abstract

Low level of dopamine (DA) in human brain may lead to neurological diseases, therefore, detection of DA is necessary. This study aims to develop 2 types of DA biosensor, i.e., electrochemical and fluorescent biosensors based on conducting polymer and quantum dot composite. The polyaniline/carbon quantum dots (PANi/CQDs) composite was prepared and characterized by UV–Vis absorption spectroscopy, fluorescence spectroscopy, FT–IR spectroscopy, scanning electron microscopy (SEM) and X–ray photoelectron spectroscopy (XPS). For electrochemical biosensor, the electrospun nanofiber film of PANi/CQDs was fabricated on fluorine doped tin oxide (FTO)–coated glass substrate. Cyclic voltammetry and amperometry were performed to study the electrochemical activity of the PANi/CQDs film toward detection of DA in neutral solution. The obtained film showed good sensitivity for DA sensing with sensitivity of 8.025 $nA.cm^{-2}.\mu M^{-1}$ and linear range of 10–90 μM ($R^2 = 0.99$) with detection limit of 0.1013 μM. In addition, for fluorescent biosensor, the fluorescent intensity of PANi/CQDs in PBS solution was quenched with increasing DA concentrations. The PANi/CQDs fluorescent biosensor presented the linear range of 0.1–100 μM ($R^2 = 0.94$) with detection limit of 0.0801 μM. The prepared PANi/CQDs composite can be promising candidate material for future use as DA biosensor in real sample analysis.

Keywords Polyaniline · Carbon quantum dots · Electrospinning · Dopamine · Biosensor

Introduction

Dopamine (DA) or 3,4–dihydroxyphenyl ethylamine is an important neurotransmitter which located in the central nervous system. Low level of DA in the central nervous is cause of several neurological diseases such as Parkinson's disease, Alzheimer and Schizophrenia [1, 2]. Recently, detection of DA by various analytical techniques, e.g., high–performance liquid chromatography [3] and gas chromatography [4] had been reported. However, the mentioned methods have some disadvantages including requirement of expensive equipment and high cost. Among the various analytical techniques used for detection of DA, the electrochemical and optical sensors have drawn much attention because of they are simple, fast, low cost, high sensitivity, and selective methods [5–7]. The graphene oxide (GO) modified glassy carbon electrode (GCE) was recently prepared electrochemical detection of DA [8]. Furthermore, the fluorescent probe based on graphitic carbon nitride (g–C_3N_4) for DA detection via fluorescent quenching was also reported [9].

Conducting polymers had received much attention for use in biomedical and sensing applications. Among the conducting polymers, polyaniline (PANi), polypyrrole (PPy), polythiophene (PTh) and their derivatives such as poly(3–aminobenzoic acid) (PABA) or poly(3,4–ethylenedioxythiophene) (PEDOT) are the common conducting polymers for sensing applications [10–12]. PANi and its derivatives are one of the most studied conducting polymers because of their excellent stability and good electronic properties [11, 12], for example, the fabricated cetyltrimethylammonium bromide (CTAB) functionalized PANi and activated charcoal (CTAB–PANi/AC) sensor had been reported for detection of DA and uric acid (UA) [13]. It was found that the CTAB–PANi/AC modified electrode showed excellent electrocatalytic activity, stability, repeatability and

✉ Saengrawee Sriwichai
saengrawee.s@cmu.ac.th

1 Department of Chemistry, Faculty of Science, Chiang Mai University, Chiang Mai 50200, Thailand

2 Graduate School, Chiang Mai University, Chiang Mai 50200, Thailand

3 Center of Excellence in Materials Science and Technology, Chiang Mai University, Chiang Mai 50200, Thailand

reproducibility to DA and UA. In addition, PANi/carbon material composites are great deal of attention materials. Carbon materials such as reduced graphene oxide (rGO) and multi–walled carbon nanotubes (MWCNTs) had been used for DA detection [14, 15]. The DA biosensor based on PANi–rGO nanocomposite showed better catalytic activity and selectivity than PANi and rGO toward the oxidation of DA. Moreover, for DA biosensor based on PANi/MWCNTs, the presence of MWCNTs could improve electrocatalytic activity of PANi electrode for DA detection. It could be therefore concluded that the presence of carbon materials could enhance the sensing performance. In addition, for other applications, composites of PANi and carbon materials such as carbon nanofiber and carbon nanotubes were applied in anti-corrosion [16, 17] and supercapacitor applications [18]. Carbon quantum dots (CQDs) are one class of carbon materials with nanometer sizes which have been used in biomedicines, optronics, sensors and catalytic applications due to their luminescent properties, high chemical stability, low toxicity and biocompatibility [6, 19–21]. Moreover, CQDs have been used for detection of DA owing to their fluorescent property and also low–cost, sensitive and selective materials. The DA biosensors based on CQDs doped with nitrogen and phosphorous [6] and carbon dots–gold nanoclusters hybrid (CDots–AuNCs) [21] had been reported. The CDots acted as the energy donor while AuNCs acted as the acceptor in fluorescence resonance energy transfer (FRET) process. The fluorescence quenching of CQDs occurred when DA was oxidized to o–quinone which could accept electrons on AuNCs surface [21]. In addition, conducting polymer/CQDs composites had been studied in various fields because of their unique physicochemical properties which led to various potential applications, i.e., biosensors, chemical sensors and supercapacitors [22–25].

Electrospinning technique has drawn much attention because of it is a simple method for producing fibers under high voltage. The obtained small size, high porosity and high surface area fibers provide benefits in various applications such as tissue engineering, targeted drug release, scaffolds, biosensors [26, 27]. However, in case of conducting polymers especially PANi, it is difficult to produce electrospun PANi fibers due to the rigid backbone and insufficient elastic properties of the PANi for electrospinning process [28]. The non–conductive polymer is therefore blended for PANi fiber formation, for example, the electrospun nanofibers of PANi blended with polyacrylonitrile (PAN) for ammonia sensor [29] and PANi blended with polystyrene for use as cholesterol biosensor [30]. In addition, electrospun composite nanofibers of silk fibroin/PAN/PANi/TiO_2 were prepared for dye removal application [31].

This study aims to develop DA biosensors i.e., electrochemical and fluorescent biosensors, based on PANi/CQDs composite. The PANi/CQDs composite was characterized by UV–Vis absorption spectroscopy, fluorescence spectroscopy, FT–IR spectroscopy, scanning electron microscopy (SEM) and X–ray photoelectron spectroscopy (XPS). Figure 1 represents schematic diagram of the developed DA biosensors. For building up the electrochemical biosensor, the electrospun nanofiber of PANi/CQDs composite was deposited on fluorine doped tin oxide (FTO)–coated glass substrate which also used as working electrode. The electrode was used for detection of DA through cyclic voltammetry and amperometry techniques at various concentrations of DA (1–90 μM). The electrospun nanofiber PANi/CQDs composite film showed a good sensitivity toward DA sensing. In addition, for fluorescent biosensor, the PANi/CQDs solution was used for detection of DA through the fluorescent quenching at various concentrations of DA (10 nM–100 μM). The fluorescent intensity of PANi/CQDs composite in PBS solution was recorded before and after addition of DA. The PANi/CQDs showed a good sensitivity and selectivity toward DA sensing. The PANi/CQDs composite is the promising candidate material for sensitive and selective sensing platform which can be future developed for use in real sample analysis.

Experimental

Materials

Polyaniline (PANi; viscosity–average molecular weight higher than 15,000, Sigma–Aldrich), poly(acrylic acid) (PAA; viscosity–average molecular weight of 450,000, Sigma–Aldrich), citric acid (Pierce), urea (AJAX), phosphate buffer saline (PBS) tablet (Sigma–Aldrich), D–glucose (Sigma–Aldrich), dopamine (Sigma–Aldrich) and ascorbic acid (Poch) were used as received without further purification. The carbon quantum dots (CQDs) were prepared according to previous study [32]. Fluorine doped tin oxide (FTO)–coated glass substrate (Sigma–Aldrich) was cleaned before use as working electrode.

Fabrication of electrospun PANi/CQDs composite fiber film

The PANi/CQDs solution was prepared by dissolving PANi (3%*w*/*v*), CQDs (1%*w*/*v*) and PAA (5% *w*/*v*) in mixed solvent of DI water and chloroform (ratio of 7:3). The solution was sonicated for 1 h and centrifuged at 4000 rpm for 1 h. The obtained solution was freshly stirred for 1 h before use for fabrication of electrospun PANi/CQDs fiber film. The optimized electrospinning condition was the voltage of 15 kV, feeding rate of 0.4 mL/h, distance between the syringe and the collector (i.e., FTO electrode) of 15 cm and period time of 1 h. The obtained PANi/CQDs composite fiber film was further used for electrochemical detection of DA.

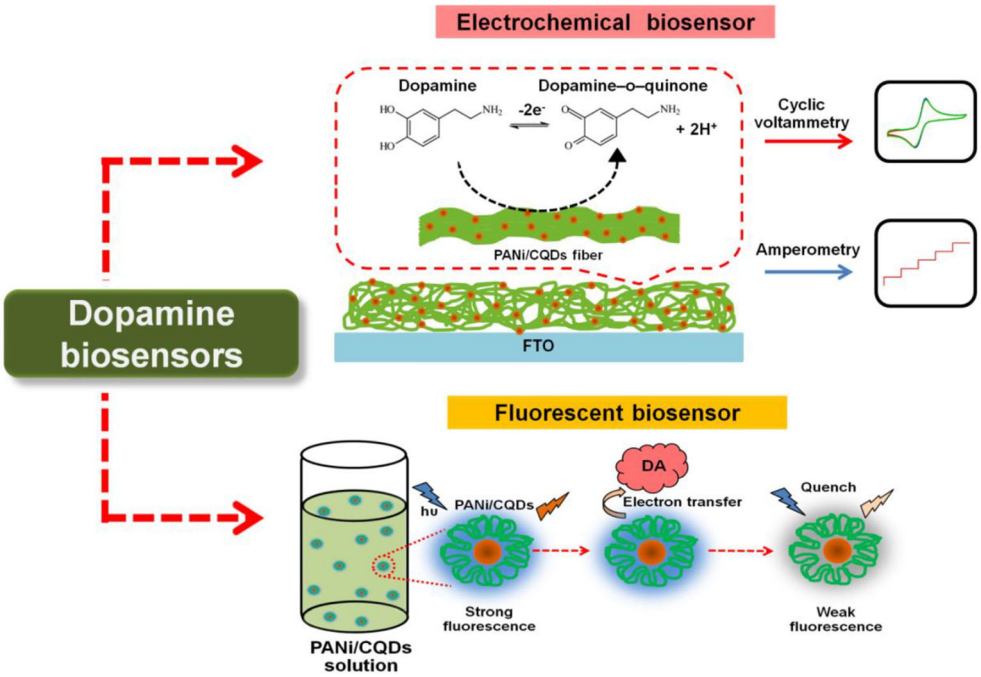

Fig. 1 Schematic diagram representing the developed electrochemical sensor and fluorescent sensor

Characterization of PANi/CQDs composite

The various characterization techniques were employed to characterize PANi/CQDs composite prior to use for DA biosensor. Particle size analyzer (HORIBA SZ–100) was employed to measure particle size of CQDs based on dynamic light scattering (DLS) measurement. In addition, particle size and surface morphology of CQDs were studied by transmission electron microscopy (TEM; JEOL JEM–2010). The X–ray diffraction (XRD; Rigaku Smartlab) analysis was also performed to confirm the formation of CQDs. The optical properties were studied using UV–Vis absorption spectroscopy (UV–1800 Shimadzu) and fluorescence spectroscopy (Synergy™ H4). The structural confirmation was investigated using FT–IR spectroscopy (Thermo Nicolet 6700 Thermoscientific) and X–ray photoelectron spectroscopy (XPS; AXIS ultra DLD spectrometer). The surface morphology of the electrospun fiber films was observed using a field emission–scanning electron microscopy (FE–SEM; JEOL JSM–6335F).

Electrochemical detection of dopamine

The electrospun PANi/CQDs composite fiber film fabricated on FTO working electrode was connected to the 3–electrode electrochemical cell with a computer control potentiostat (eDAQ: ED410 e–corder 410). The reference electrode was Ag/AgCl (in 3 M KCl) and counter electrode was platinum wire. The sensing experiment was performed by adding various concentrations of DA (10–90 μM) into PBS solution and monitored using cyclic voltammetry with potential range of −0.2 V to 0.8 V at scan rate of 20 mV/s. In addition, the amperometric responses of the DA biosensor based on electrospun PANi/CQDs composite fiber were obtained by successive addition of various concentrations of DA (1–90 μM) into PBS solution at constant applied potentials of 0.38 V. Cyclic voltammetry at various scan rates (20, 40, 60, 80, 100, 200, 300 and 400 mV/s) was performed using 90 μM DA in PBS solution under applied potential of −0.2 V to 0.8 V. For selectivity experiment, ascorbic acid and glucose were further employed in both cyclic voltammetry and amperometry.

Fluorescence detection of dopamine

The PANi (0.10%*w*/*v*) and CQDs (0.020%*w*/*v*) composite was prepared in PBS solution for detection of DA (10 nM–100 μM). The fluorescence spectra were immediately recorded with an excitation wavelength at 360 nm after addition of DA.

Results and discussion

Characterization of PANi/CQDs composite

TEM image of the synthesized CQDs dispersed in water is shown in Fig. 2a with average diameter of 11.8 ± 2.9 nm. The DLS measurement indicated that average diameter of CQDs was about 9–10 nm (result is not shown). The XRD pattern of the obtained CQDs is shown in Fig. 2b. The CQDs exhibited a broad peak at an angle of $2\theta = 19.2°$ which indicated

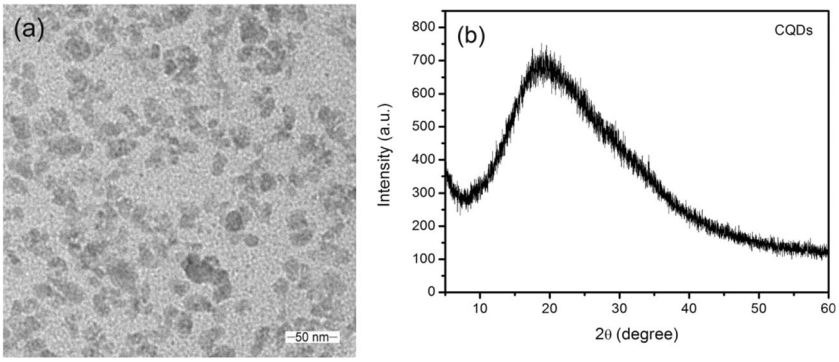

Fig. 2 **a** TEM image and **b** XRD pattern of CQDs

amorphous carbon in nature [33, 34]. The optical properties of the CQDs and PANi/CQDs were examined by UV–Vis absorption spectroscopy and fluorescence spectroscopy. The absorption spectra of CQDs, PANi and PANi/CQDs in DI water are shown in Fig. 3. The PANi showed absorption peak at 260 nm which corresponded to π–π* transition from the benzene ring [35]. The CQDs represented absorption peaks at 291 nm and 343 nm which related to π–π* and n–π* transitions from aromatic C=C bond and C=O bond, respectively [36, 37]. The UV–Vis spectrum of PANi/CQDs composite was mainly similar to PANi and CQDs which showing peaks at 285 nm and 354 nm due to the π–π * transition in the benzenoid ring and n–π* transition of C=O bond, respectively [35, 37]. The absorption peak of n–π* transition of C=O bond in PANi/CQDs composite was red shifted due to the interaction of CQDs and polymer (PANi) matrix [32].

The fluorescence intensity is dependent on the excitation wavelength [32]. The CQDs and PANi/CQDs solutions were excited in the range of 340–380 nm which showed the emission fluorescence peaks in the range of 405–445 nm. The maximum emission intensity was clearly observed at excitation wavelength of 360 nm with an emission peak of 426 nm as shown in Fig. 4. This excitation wavelength was selected for performing fluorescent DA biosensor afterward. The fluorescence intensities of CQDs were obviously high at all excitation wavelengths. Furthermore, the fluorescence intensities of PANi/CQDs composite were obviously observed to be higher than that of the PANi which implied to the incorporation of CQDs into PANi. This circumstance could be explained as the nitrogen dopant in CQDs structure played important role to exhibit photoluminescence properties which could enhance the emission of the CQDs by increasing the fermi level and electrons in the conduction band. Moreover, the direct recombination of excited electrons from the n–π* transition of C=O and C=N groups can also lead to the emission of CQDs [32]. The blue shifting emission was also observed with increasing excitation wavelength. This shifting might be the result of the size distribution of the prepared CQDs which led to the different energy trapping upon excitation wavelength [38, 39].

FT–IR spectroscopy was utilized to analyze the functional groups of PAA, PANi, CQDs and PANi/CQDs films. The FT–IR spectra of PAA, PANi, CQDs and PANi/CQDs films are shown in Fig. 5. The PAA represented the peaks at 1697 and 1450 cm^{-1} which were assigned to the stretching vibration of COOH and bending vibration of COO, respectively [32]. The peaks of PANi at 2800–2900, 1556, 1453 and 1299 cm^{-1}

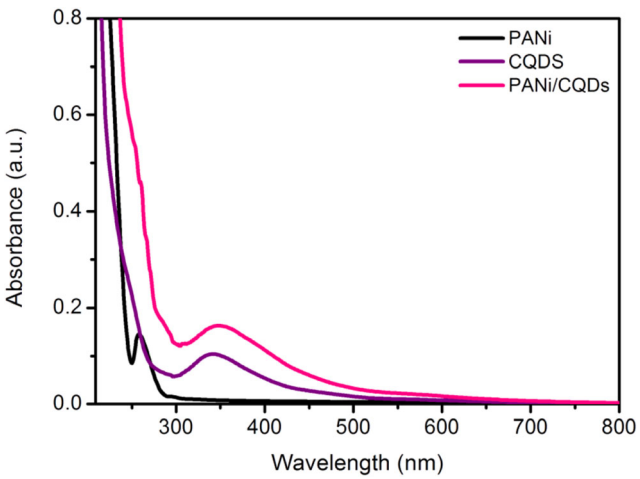

Fig. 3 UV–Vis absorption spectra of CQDs, PANi and PANi/CQDs in DI water

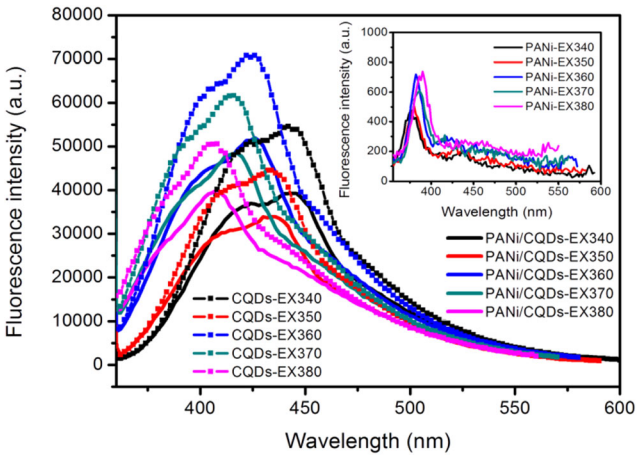

Fig. 4 Fluorescence spectra of PANi, CQDs and PANi/CQDs in PBS solution at excitation wavelengths of 340–380 nm (EX340–EX380). Inset shows the expanded fluorescence spectra of PANi

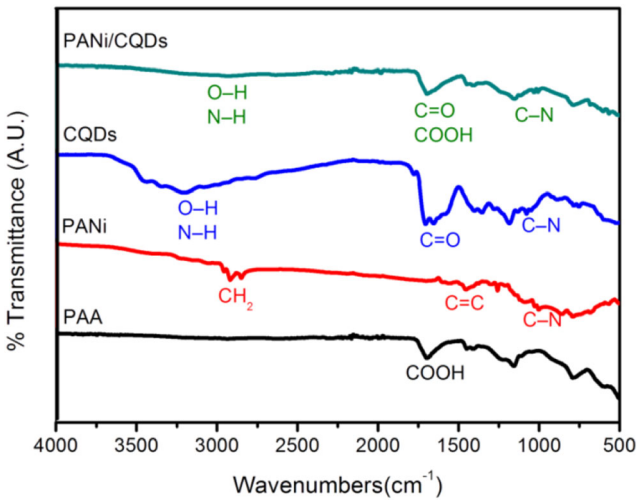

Fig. 5 FT–IR spectra of PAA, PANi, CQDs and PANi/CQDs films

corresponded to the to $–CH_2$ and –CH, C=C stretching of quinoid rings, C=C stretching vibration of benzenoid rings and C–N stretching of benzenoid unit, respectively [23, 40, 41]. The broad band at 3100–3500 cm^{-1} attributed to O–H and N–H group in CQDs whereas the peaks at 1077 and 1655 cm^{-1} were assigned to C–N stretching and C=O stretching of carboxylic group on the surface, respectively [23, 36]. The FT–IR spectrum of PANi/CQDs composite film showed the broad band of O–H, N–H and CH_2 stretching at around 3000 cm^{-1}. The broad peak of C=O stretching in CQDs and COOH of PAA was represented about 1695 cm^{-1} whereas the peak of C–N stretching of PANi and CQDs was shown at 1032 cm^{-1}. However, the presence of both PANi and CQDs in the composite fiber film was not clearly observed. The another characterization technique, i.e., XPS was then employed to confirm the presence of PANi/CQD composite.

XPS measurement was further performed to study the chemical composition of the films. The XPS spectra of the PANi, PAA, CQDs and PANi/CQDs films are presented in Fig. 6. The survey spectra in Fig. 6a represented the peaks of C1s, N1s and O1s at ~285 eV, 400 eV and 532 eV for PANi, CQDs, and PANi/CQDs film. In case of PAA, only C1s and O1s peaks were observed. For PANi, the presence of oxygen was probably associated with contamination produced during the preparing process. This contamination could be also caused by the environmental contact and water adsorption upon storage [42, 43]. The high resolution C1s and N1s spectra of CQDs film are shown in Fig. 6b. The C1s peaks at binding energy of 284.9 eV, 285.6 eV, 287.1 eV and 289.0 eV were contributed to C=C or C–C, C–OH or C–O–C, C–O or C–N and O–C=O, respectively. For N1s peaks, the C–N and N–H or C=N functional groups were shown at 400.2 eV and 402.1 eV, respectively [37, 42, 44, 45]. The high resolution C1s and N1s spectra of the PANi film were presented in Fig. 6c. The XPS spectrum for C1s indicated the presence of benzenoid structure in PANi, i.e., C–N or C=N at 284.9 eV and $C–N^+$ or $C=N^+$ at 285.8 eV. The peak of

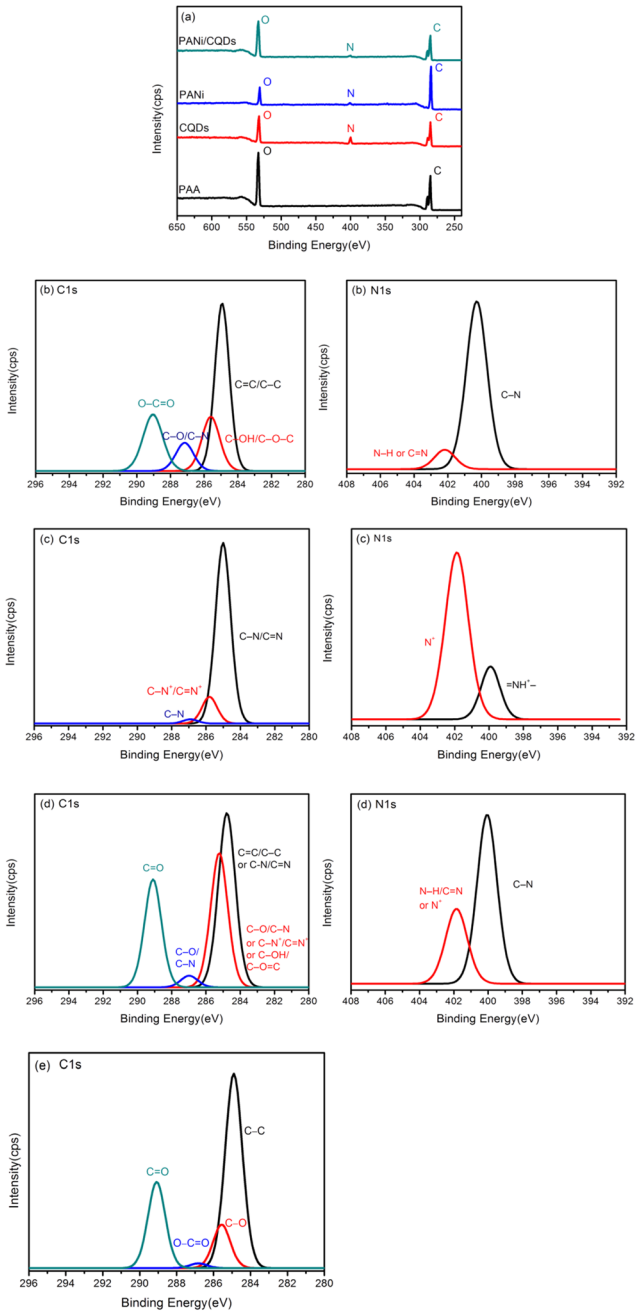

Fig. 6 XPS **a** survey spectra and high resolution spectra of **b** CQDs, **c** PANi, **d** PANi/CQDs and **e** PAA films

cationic specie of nitrogen ($=NH^+–$) was also observed at 399.6 eV. The nitrogen contribution at 401.7 eV can be assigned to positively charged nitrogen (N^+) which representing the formation of the protonated nitrogen specie [42, 45]. The high resolution spectra of the PANi/CQDs film are presented in Fig. 6d. The C1s peaks at 284.2 eV, 285.2 eV, 286.9 eV and 289.0 eV were assigned to C–C or C=C, C–N or C=N, C–O or C–N, C–N^+ or C=N^+, C–OH or C–O=C, C–O and C=O, respectively, of PAA, PANi and CQDs. The N1s peak at 400.0 eV and 401.8 eV were assigned to C–N and N–H or C=N or N^+ from PANi and

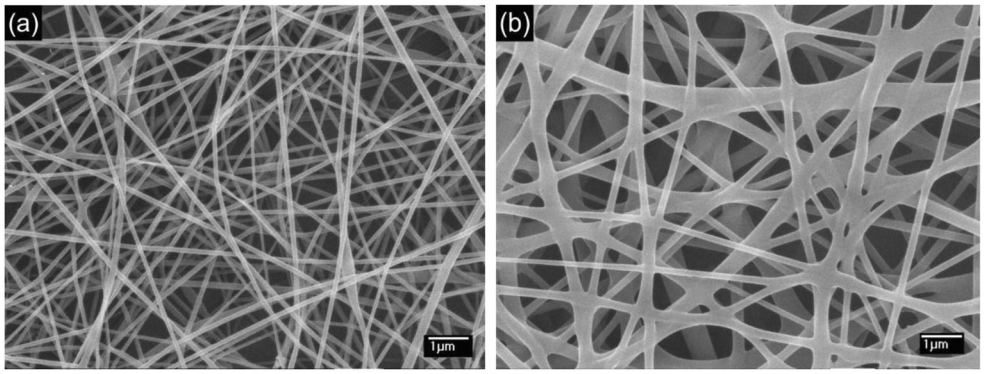

Fig. 7 FE–SEM images of **a** PANi and **b** PANi/CQDs electrospun fibers

CQDs. Moreover, PAA was blended with PANi/CQDs for manufacturing electrospun fiber in this study. The C1s high resolution spectrum of PAA is shown in Fig. 6e. The peaks at 284.7 eV, 285.2 eV, 286.5 eV and 289.0 eV were assigned to C–C, C–O, C=O and O–C=O species, respectively [44, 45]. From XPS survey spectra, the atomic percentage of nitrogen in CQDs, PANi and PANi/CQDs films were calculated to be 8.14%, 2.08% and 2.49%, respectively. The higher percentage of nitrogen in PANi/CQDs film than that of the PANi film indicated the presence of CQDs in the electrospun PANi/CQDs fiber film [32].

It is difficult to obtain the PANi or other conducting polymer fibers by electrospinning method due to their rigid backbones. In addition, their high degree of aromaticity lead the elastic properties of the solution insufficient for electrospinning [27, 29]. Therefore, PAA as a non–conductive polymer was selected for blending with PANi/CQDs for formation of electrospun fiber in this work. Surface morphology of the obtained PANi and PANi/CQDs electrospun fibers was examined by FE–SEM as shown in Fig. 7. It can be seen that the surfaces of PANi and PANi/CQDs fibers were uniform and smooth. The average diameters of PANi and PANi/CQDs fibers were calculated to be 120 nm and 320 nm, respectively. The increasing of PANi/CQDs fiber size was due to the addition of CQDs in PANi to form PANi/CQDs composite [46].

Electrochemical detection of dopamine

In this study, the electrospun PANi/CQDs fiber was employed for fabrication of an electrochemical DA biosensor. The electrospinning is convenient method for producing fiber under a high applied voltage between a metal needle and a collector. The polymer solution is jetted from the metal needle to deposit on FTO electrode as a collector [27]. The employed electrospinning condition was optimized prior to fabricate the DA biosensor. Cyclic voltammetry was performed to study the electrochemical activity of PANi and PANi/CQDs toward

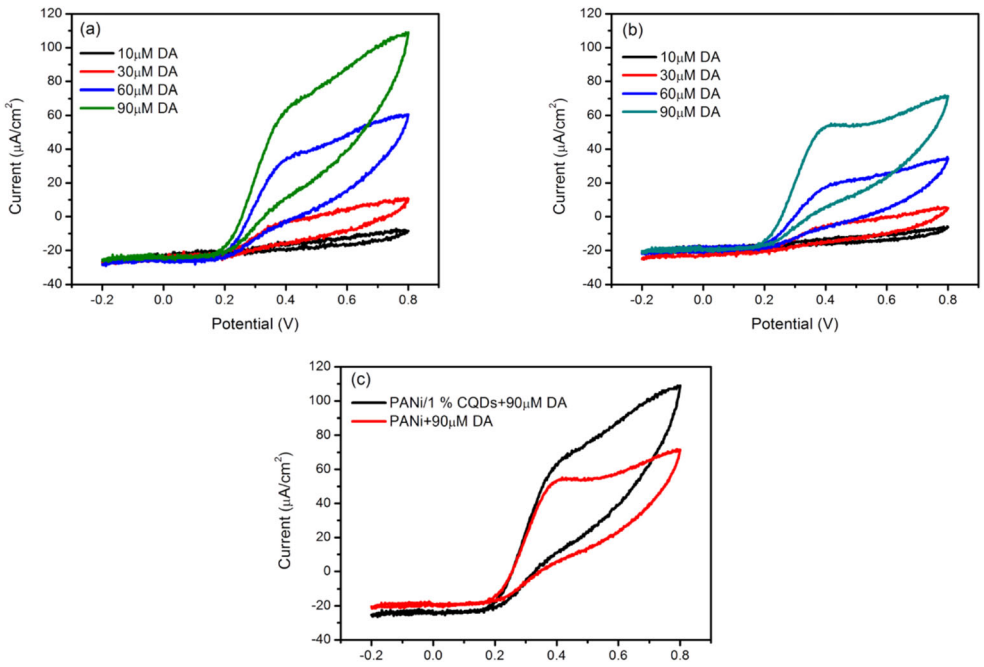

Fig. 8 Cyclic voltammograms of **a** PANi/CQDs and **b** PANi toward detection of 10–90 μM DA in PBS solution **c** cyclic voltammograms of PANi and PANi/CQDs for detection of 90 μM DA

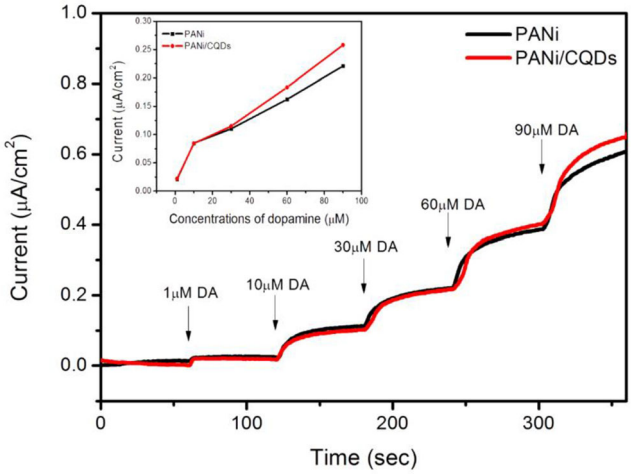

Fig. 9 Amperometric responses of PANi and PANi/CQDs film with successive addition of 1–90 μM DA to PBS solution at 0.38 V

various concentrations of DA (10–90 μM) at scan rate of 20 mV/s and potential range of −0.2 V to 0.8 V in neutral PBS solution. The cyclic voltammograms of PANi and PANi/CQDs for detection of DA (10–90 μM) are shown in Fig. 8a and b, respectively. The current responses of both electrodes increased with increasing concentrations of DA. For comparison, the cyclic votammograms of PANi and PANi/CQDs toward detection of 90 μM DA are shown in Fig. 8c. The current response of PANi/CQDs upon detection of DA was obviously higher than that of PANi due to the abundant surface functional groups, i.e., hydroxyl, carboxyl and amine groups, of CQDs could interact with the DA molecule through π–π stacking and hydrogen bonding interactions [6, 19].

As seen in Fig. 8, the anodic peaks of cyclic voltammograms for DA sensing were observed at 0.38 V. The constant applied potential for the amperometric experiment at 0.38 V was therefore selected. The amperometric responses of PANi and PANi/CQDs in PBS are shown in Fig. 9. The current responses of PANi and PANi/CQDs were increased upon successive addition of DA (1–90 μM) due to the oxidation of DA on PANi and PANi/CQDs surfaces was increased. This situation could be explained as the increasing of π–π interaction between phenyl structure of DA and benzenoid structure of PANi [47]. Moreover, the hydroxyl, carboxyl and amine groups of CQDs could interact with DA through π–π stacking and hydrogen bonding interactions [6].

The current response of PANi/CQDs was slightly higher than that of PANi. The sensitivity of electrochemical DA biosensor was calculated from slope of amperometric curve (μA) and concentration of DA as shown in the inset of Fig. 9 [48]. The sensitivities of PANi and PANi/CQDs were calculated to be 7.587 and 8.025 nA.cm^{-2}.μM^{-1}, respectively, with limit of

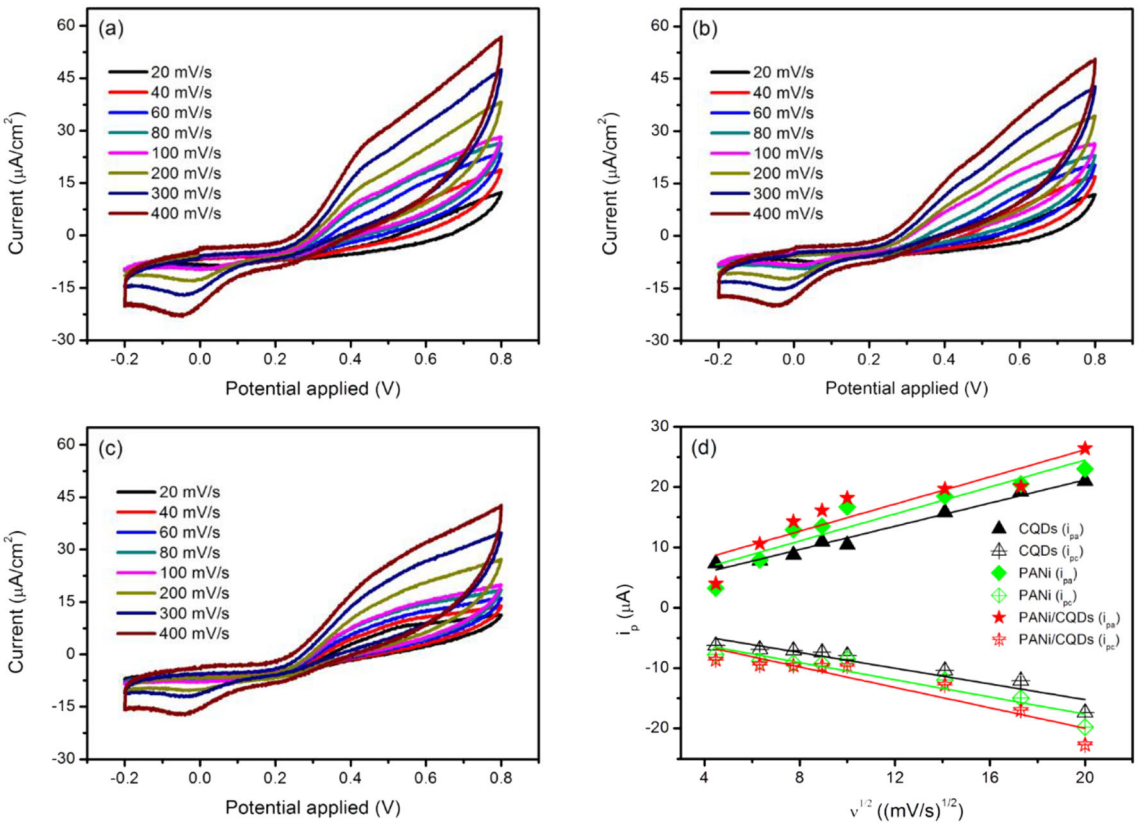

Fig. 10 Cyclic voltammograms **a** PANi/CQDs **b** PANi **c** CQDs performed in 90 μM DA in PBS solution at different scan rates and **d** linear relationship between i_p vs. $\nu^{1/2}$

Table 1 Electroactive areas (A, in mm^2) of different electrodes, calculated from the CV scans performed in 90 μM DA in PBS solution

	CQDs	PANi	PANi/CQDs
A_{anodic}	0.962	1.12	1.127
$A_{cathodic}$	0.652	0.714	0.848

detection (LOD) of 0.2089 μM for PANi and 0.1013 μM for PANi/CQDs and linear range of 10–90 μM ($R^2 = 0.99$). The LOD was calculated from the slope of the above mentioned curves and the standard deviation of amperometric responses of PBS blank solution. The sensitivity and LOD were observed to be enhanced for PANi/CQDs electrode. The results of cyclic voltammetry and amperometry demonstrated that the CQDs could improve the electrocatalytic activity of PANi towards detection of DA. The cyclic voltammograms for detection of 90 μM DA in PBS solution under applied potential range of −0.2 V to 0.8 V at different scan rates using different electrodes with linear relationship plots of anodic current peak height (i_{pa}) and cathodic current peak height (i_{pc}) versus square root of the scan rate ($\nu^{1/2}$) are shown in Fig. 10. The linear relationship confirms the diffusion control at the electrode surface. The electrochemical surface area (A) of CQD, PANi and PANi/CQDs electrodes was calculated from Randles-Sevcik equation at the angular coefficient of the linear plots of current peak height (i_p) versus $\nu^{1/2}$ [49]. Table 1 represents the calculated electrochemical surface area of both anodic (A_{anodic}) and cathodic ($A_{cathodic}$) scans of different electrodes.

Furthermore, the selectivity experiment of PANi/CQDs electrode was performed by amperometric method and cyclic voltammetry toward common interferences, i.e., glucose (Glc) and ascorbic acid (AA). The amperometric response at 0.38 V and cyclic voltammogram of PANi/CQDs with successive addition of DA, Glc and AA into PBS solution are shown in Fig. 11. The current responses of PANi/CQDs electrode towards detection of DA were obviously higher than that of the responses of the interferences. The AA could perform the electrochemical oxidation toward detection of DA at 0.2–0.4 V, however, AA could form negatively charge in neutral PBS solution which led to electrostatic repulsion between the negatively charged oxygen functional groups (COO^-) of PAA and CQDs at pH 7 [50]. For detection of glucose, the PANi/CQDs could not respond toward addition of Glc due to the absence of glucose oxidase catalyst for glucose detection [51]. The results implied that the developed electrochemical DA biosensor based on electrospun PANi/CQDs composite fiber film presenting high selectivity.

Fluorescence detection of dopamine

It is well–known that CQDs exhibit fluorescence properties [19, 22]. We therefore employed PANi/CQDs composite for detection of DA in this study. As we observed in Fig. 4, the fluorescence intensities of PANi were very low with noise signal therefore the PANi would not be chosen for detection of DA. The fluorescent DA biosensor based on PANi/CQDs composite was used for detection of DA (10 nM–100 μM) in neutral PBS solution. Figure 12 shows fluorescence spectra of PANi/CQDs composite upon detection of DA and interferences at excitation wavelength of 360 nm. The maximum emission peaks were located at about 442 nm. The fluorescence quenching was observed after adding the substances into PBS solution. As shown in Fig. 12a, the fluorescent intensity of the PANi/CQDs decreased gradually with the increasing of DA concentrations (10 nM–100 μM). The PANi/CQDs fluorescent biosensor presented the the linear range of 0.1–100 μM ($R^2 = 0.94$) with detection limit of 0.0801 μM. The quenching mechanism of CQDs could be explained as the oxidized DA or dopamine–quinone could quench the fluorescence of CQDs. As the result, the higher concentration of DA therefore led to more quenching effect of CQDs. In addition, hydroxyl, carboxyl and amine groups of CQDs could interact with DA through π–π stacking and hydrogen bonding interactions [6]. PANi could also interact with DA through π–π interaction between phenyl structures of DA and PANi [47]. These interactions led to enhancement the quenching effect of CQDs in PANi/CQDs composite toward detection of DA. The fluorescence spectra upon detection of DA using CQDs and PANi/CQDs are shown in Fig. 12b. Upon sensing with 100 nM DA, the PANi/CQDs composite showed more fluorescence quenching than CQDs. The selectivity of the PANi/CQDs was investigated by sensing with Glc and AA as

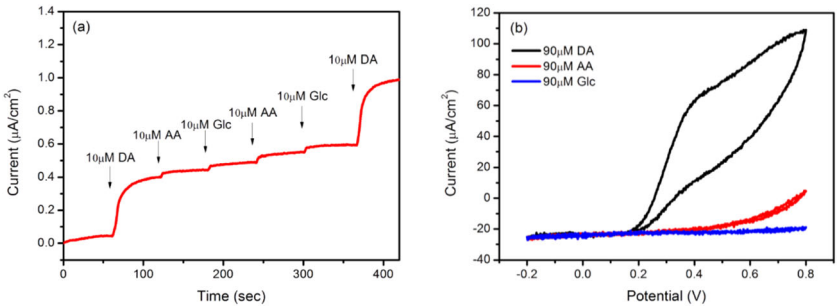

Fig. 11 Electrochemical responses of PANi/CQDs biosensor **a** amperometric response with successive addition of DA, AA and Glc at 0.38 V and **b** cyclic voltammograms toward detection of 90 μM of DA, AA and Glc in PBS solution

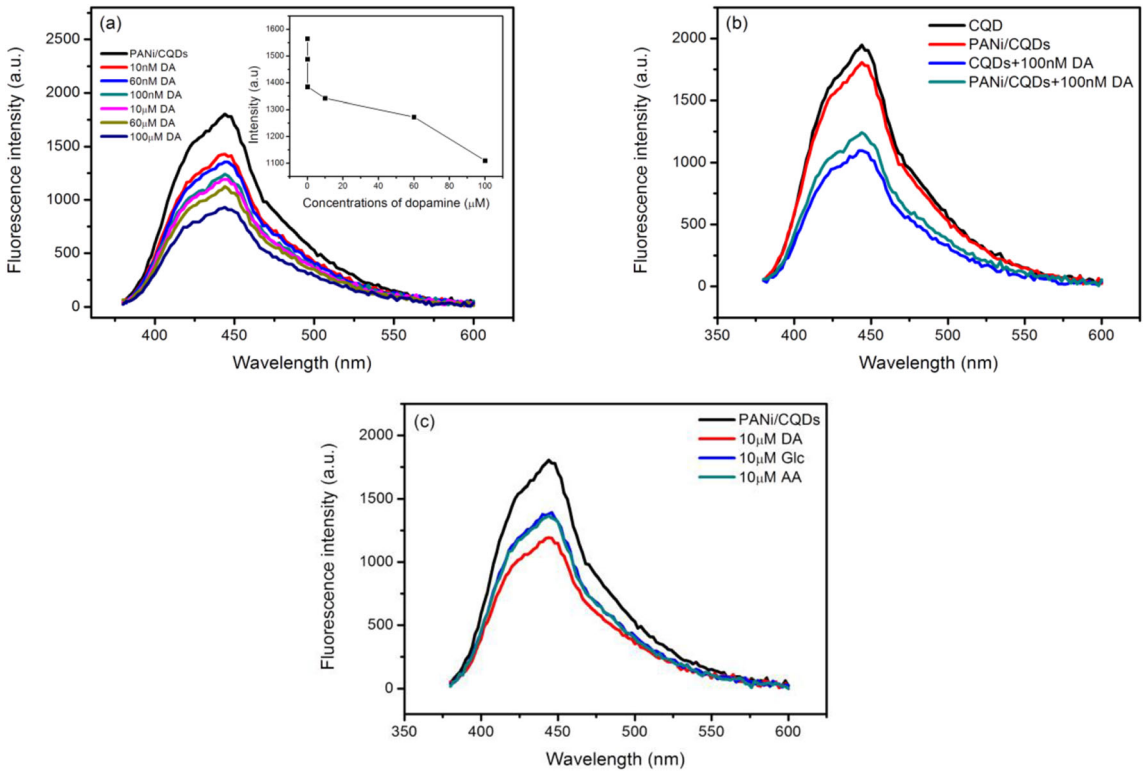

Fig. 12 Fluorescence quenching of PANi/CQDs with addition of **a** various concentrations of DA, **b** fluorescence quenching of PANi/CQDs and CQDs with addition of 100 nM DA and **c** 10 μM of DA, AA and Glc

represented in Fig. 12c. The fluorescence quenching was obviously seen after adding DA whereas the quenching could be slightly observed upon adding both Glc and AA. These results implied that the PANi/CQDs composite represented the great potential and ability for DA detection by fluorescence quenching.

Table 2 shows the comparison of some previous CQDs–based works for detection of DA. It can be concluded from the

Table 2 Summary of fluorescent and electrochemical biosensors for detection of DA

Types of sensor	Linear range (μM)	Limit of detection (μM)	Sensitivity	Ref.
Fluorescent biosensor				
N, P doped CQDs	10–500	0.021	–	[6]
CDs/TYR	0.206–131.8	0.06	–	[7]
CDots–AuNCs	0.005–0.180	0.0029	–	[21]
CDs/CuNCs nanohybrids	0.1–100	0.032	–	[52]
N–CQDs	0.1–200	0.05	–	[53]
PANi/CQDs	0.1–100	0.0801	–	This work
Electrochemical biosensor				
MoS_2–PANi/rGO/GCE	5.0–500	0.70	–	[54]
GCE modified with CQDs	0.19–11.81	2.7	9.3 (mA μM^{-1})	[55]
AuNPs@PANi/GSPE	1–100	0.86	–	[56]
Fe–Meso–PANi	10–300	9.8	0.2693(μA/μM)	[57]
GO–PANi/GCE	1–14	0.5	–	[58]
PANi/CQDs	10–90	0.1013	8.025 ($nA.cm^{-2}.\mu M^{-1}$)	This work

Abbreviation: *N, P doped CQDs* nitrogen and phosphorous doped carbon quantum dots, *CDs/TYR* carbon dots/tyrosinase, *CDots–AuNCs* carbon dots–gold nanoclusters hybrid, *CDs* carbon dots, *CuNCs* copper nanoclusters, *N–CQDs* Nitrogen-doped carbon quantum dots, *rGO* reduced graphene oxide, *MoS_2* molybdenum disulfide, *GCE* glassy carbon electrodes, *GSPEs* graphite screen-printed electrodes, *AuNPs* gold nanoparticles, *Fe–Meso–PANi* Fe ion-exchanged mesoporous polyaniline, *GO* graphene oxide

results of electrochemical and fluorescence DA biosensors based on PANi/CQDs composite that the developed DA biosensors presented the ability for detection of low concentration of DA with good sensitivity and high selectivity. Detection of low concentration of DA is importance because low level of DA can be used to indicate the neurological diseases [59]. Therefore, development of DA biosensor is necessary for detection of DA at low concentration.

Conclusions

The electrochemical and fluorescent DA biosensors based on PANi/CQDs composite were successfully developed for detection of low concentration of DA. The PANi/CQDs composite was prepared and characterized prior to use for building up the DA biosensors. For electrochemical biosensor, the electrospun fiber film of PANi/CQDs composite was fabricated on FTO substrate which also used as working electrode for electrochemical detection of DA. The electrochemical detection of DA was performed using cyclic voltammetry and amperometry at various concentrations of DA (1–100 μM). The obtained electrospun PANi/CQDs fiber film exhibited good selectivity and high sensitivity toward DA sensing. For fluorescent biosensor, the PANi/CQDs solution was used for detection of various concentrations of DA (10 nM–100 μM) through fluorescent quenching. The PANi/CQDs composite showed a good sensitivity toward DA sensing. The PANi/CQDs composite is the promising candidate material for sensitive and selective detection of DA which becomes a sensing platform for future use in real sample analysis.

Acknowledgments The work was supported by the Center of Excellence in Materials Science and Technology, Chiang Mai University. The authors would like to acknowledge Faculty of Medicine, Chiang Mai University for photoluminescence measurement.

References

1. Vulto AG, Westenberg HG, Meijer LB, Versteeg DH (1986) The Dopamine Metabolite 3-Methoxytyramine Is Not a Suitable Indicator of Dopamine Release in the Rat Brain. J Neurochem 45: 1387–1393
2. Diab N, Morales DM, Andronescu C, Masoud M, Schuhmann W (2019) A sensitive and selective graphene/cobalt tetrasulfonated phthalocyanine sensor for detection of dopamine. Sensors Actuators B Chem 285:17–23
3. Carrera V, Sabater E, Vilanova E, Sogorb MA (2007) A simple and rapid HPLC–MS method for the simultaneous determination of epinephrine, norepinephrine, dopamine and 5-hydroxytryptamine: Application to the secretion of bovine chromaffin cell cultures. J Chromatogr B 847:88–94
4. Naccarato A, Gionfriddo E, Sindona G, Tagarelli A (2014) Development of a simple and rapid solid phase microextraction-gas chromatography–triple quadrupole mass spectrometry method for the analysis of dopamine, serotonin and norepinephrine in human urine. Anal Chim Acta 810:17–24
5. Venton BJ, Wightman RM (2003) Psychoanalytical Electrochemistry: Dopamine and Behavior. Anal Chem 1:414–41A
6. Tammina SK, Yang D, Koppala S, Chengsheng C, Yang Y (2019) Highly photoluminescent N, P doped carbon quantum dots as a fluorescent sensor for the detection of dopamine and temperature. J Photochem Photobiol B Biol 194:61–70
7. Li H, Liu J, Yang M, Kong W, Huang H, Liu Y (2014) Highly sensitive, stable, and precise detection of dopamine with carbon dots/tyrosinase hybrid as fluorescent probe. RSC Adv 4:46437–46443
8. Gao F, Cai X, Wang X, Gao C, Liu S, Gao F, Wang Q (2013) Highly sensitive and selective detection of dopamine in the presence of ascorbic acid at graphene oxide modified electrode. Sensors Actuators B Chem 186:380–387
9. Lv J, Feng S, Ding Y, Chen C, Zhang Y, Lei W, Hao Q, Chen SM (2019) A high-performance fluorescent probe for dopamine detection based on g-C3N4 nanofibers. Spectrochim Acta A 212:300–307
10. Megha R, Ali FA, Ravikiran YT, Ramana C, Kumar ABVK, Mishra DK, Vijayakumari SC, Kim D (2018) Conducting polymer nanocomposite based temperature sensors: A review. Inorg Chem Commun 98:11–28
11. Mathiyarasu J, Senthilkumar S, Phani KLN, Yegnaraman V (2005) Selective detection of dopamine using a functionalised polyaniline composite electrode. J Appl Electrochem 53:513–519
12. Zuo F, Jin L, Fu X, ZhangH YR, Chen S (2017) An electrochemiluminescent sensor for dopamine detection based ona dual-molecule recognition strategy and polyaniline quenching. Sensors Actuators B Chem 244:282–289
13. Govindasamy M, Chen SM, Mani V, Sathiyan A, Merlin JP, Al-Hemaid FMA, Ali MA (2016) Simultaneous determination of dopamine and uric acid in presence of high concentration of ascorbic acid using cetyltrimethylammonium bromide–polyaniline/activated charcoal composite. RSC Adv 6:100605–100613
14. Xie LQ, Zhang YH, Gao F, Wu QA, Xu PY, Wang SS, Gao NN, Wang QX (2017) A highly sensitive dopamine sensor based on a polyaniline/reduced graphene oxide/Nafion nanocomposite. Chin Chem Lett 28:41–48
15. Sabzi RE, Rezapour K, Samadi N (2010) Polyaniline-multi-wall-carbon nanotube nanocomposites as a dopamine sensor. J Serb Chem Soc 75:537–549
16. Yuan R, Liu H, Yu P, Wang H, Liu J (2018) Enhancement of adhesion, mechanical strength and anti-corrosion by multilayer superhydrophobic coating embedded electroactive PANI/CNF nanocomposite. J Polym Res 25(7):151
17. Jafari Y, Ghoreishi SM, Shabani-Nooshabadi M (2016) Preparation of covalently bonded polyaniline nanofibers/carbon nanotubes supercapacitor electrode materials using interfacial polymerization approach. J Polym Res 23:91
18. Xiong S, Zhang X, Wang R, Lu Y, Li H, Liu J, Li S, Qui Z, Wu B, Chu J, Zhang R, Gong M, Chen Z, Wang X (2019) Preparation of covalently bonded polyaniline nanofibers/carbon nanotubes supercapacitor electrode materials using interfacial polymerization approach. J Polym Res 26(4):90
19. Hu A, Wang Y (2014) Carbon quantum dots: synthesis, properties and applications. J Mater Chem C 2:6921–6939
20. Yang S, Sun X, Wang Z, Wang X, Guo G, Pu Q (2017) One-step facile green synthesis of a highly fluorescent molecule through a way towards carbon dots and detection of dopamine based on in-situ formation of silver nanoparticles. Sensors Actuators B Chem 253:752–758
21. He YS, Pan CG, Cao HX, Yue MZ, Wang L, Liang GX (2018) Highly sensitive and selective dual-emission ratiometric

fluorescencedetection of dopamine based on carbon dots-gold nanoclusters hybrid. Sensors Actuators B Chem 256:371–377
22. Chung TS, Zhao DL (2018) Applications of Carbon Quantum Dots (CQDs) in Membrane Technologies: A Review. Water Res 147: 43–49
23. Gao F, Du X, Hao X, Li S, An X, Liu M, Han N, Wang T, Guan G (2017) An electrochemically-switched BPEI-CQD/PPy/PSS membrane for selective separation of dilute copper ions from wastewater. Chem Eng J 328:293–303
24. Uthirakumar P, Devendiran M, Yun JH, Kim GC, Kalaiarasan S, Lee IH (2018) Role of carbon quantum dots and film thickness on enhanced UV shielding capability of flexible polymer film containing carbon quantum dots/N-doped ZnO nanoparticles. Opt Mater 84:771–777
25. Xie Y, Zhao Z (2017) Enhanced electrochemical performance of carbon quantum dots-polyaniline hybrid. J Power Sources 337:54–64
26. Kamble P, Sadarani B, Majumdar A, Bhullar S (2017) Nanofiber based drug delivery systems for skin: A promising therapeutic approach. J Drug Deliv Sci Technol 41:124–133
27. Lee JKY, Chen N, Peng S, Li L, Tian L, Thakor N, Ramakrishna S (2017) Polymer-based composites by electrospinning: Preparation & functionalization with nanocarbons. Prog Polym Sci 41:40–84
28. Bhardwaj N, Kundu SC (2010) Electrospinning: A fascinating fiber fabrication technique. Biotechnol Adv 28:325–347
29. Anwane RS, Kondawar SB, Late DJ (2018) Bessel's polynomial fitting for electrospun polyacrylonitrile/Polyaniline blend nanofibers based ammonia sensor. Mater Lett 211:70–73
30. Shin YJ, Kameoka QJ (2018) Amperometric cholesterol biosensor using layer-by-layer adsorption technique onto electrospun polyaniline nanofibers. J Ind Eng Chem 18:193–197
31. Aziz S, Sabzi M, Fattahi A, Arkan E (2017) Electrospun silk fibroin/PAN double-layer nanofibrous membranes containing polyaniline/TiO2 nanoparticles for anionic dye removal. J Polym Res 24(9):140
32. Alam AM, Liu Y, Park M, Park SJ, Kim HY (2015) Preparation and characterization of optically transparent and photoluminescent electrospun nanofiber composed of carbon quantum dots and polyacrylonitrile blend with polyacrylic acid. Polymer 59:35–41
33. Luo K, Jiang X (2019) Fluorescent Carbon Quantum Dots with Fe(III/II) Irons as Bridge for the Detection of Ascorbic Acid and H2O2. J Fluoresc 29(3):769–777
34. Wu F, Su H, Wang K, Wong WK, Zhu X (2017) Facile synthesis of N-rich carbon quantum dots from porphyrins as efficient probes for bioimaging and biosensing in living cells. J Nanomed 12:7375–7391
35. Huang WS, MacDiarmid AG (1993) Optical properties of polyaniline. Polymer 34:1833–1845
36. Wang L, Liu X, Lu Q, Wang X, Qu S (2012) A Biocompatible Fluorescent Ink Based on Water-Soluble Luminescent Carbon Nanodots. Angew Chem Int Ed 51:12215–12218
37. Tang J, Zhang J, Zhang Y, Xiao Y, Shi Y, Chen Y, Ding L, Xu W (2019) Influence of Group Modification at the Edges of Carbon Quantum Dots on Fluorescent Emission. Nanoscale Res Lett 14: 241
38. Wang F, Pang S, Wang L, Li Q, Kreiter M, Liu CY (2010) One-Step Synthesis of Highly Luminescent Carbon Dots in Noncoordinating Solvents. Chem Mater 22:4528–4530
39. Shi Y, Pan Y, Zhang H, Zhang Z, Li MJ, Yi C (2014) A dual-mode nanosensor based on carbon quantum dots and gold nanoparticles for discriminative detection of glutathione in human plasma. Biosens Bioelectron 56:39–45
40. Bera S, Kundu S, Khan H, Jana S (2018) Polyaniline coated graphene hybridized SnO2 nanocomposite: Low temperature solution synthesis, structural property and room temperature ammonia gas sensing. J Alloys Compd 744:260–270
41. Zhang D, Wu Z, Li P, Zong X, Dong G, Zhang Y (2018) Facile fabrication of polyaniline/multi-walled carbon nanotubes/molybdenum disulfide ternary nanocomposite and its high-performance ammonia-sensing at room temperature. Sensors Actuators B Chem 258:895–905
42. Golczak S, Kanciurzewska A, Fahlman M, Langer K, Langer JJ (2008) Comparative XPS surface study of polyaniline thin films. Solid State Ionics 179:2234–2239
43. Parra ER, Arango PJA, Palacio VJB (2010) XPS structure analysis of TiN/TiC bilayers produced by pulsed vacuum arc discharge. Dyna 163:64–74
44. Li Q, Mao D, Li D, Chen Y, Chen X, Xu X (2018) A versatile porous 3D polyurethane/polyacrylic acid (PU-PAA) membrane for one-step multiple contaminants water purification. J Membr Sci 563:191–198
45. Kim HB, Park JA, Kang JK, Lee SC (2017) Electrospun poly(acrylic acid)/poly(vinyl alcohol) nanofibrous adsorbents for Cu(II) removal from industrial plating wastewater. RSC Adv 7:18075–18084
46. Zhang P, Zhao X, Ji Y, Ouyang Z, Wen X, Li J, Su Z, Wei G (2015) Electrospinning graphene quantum dots into a nanofibrous membrane for dual-purpose fluorescent and electrochemical biosensors. J Mater Chem B 3:2487–2496
47. Yang L, Liu S, Zhang Q, Li F (2012) Simultaneous electrochemical determination of dopamine and ascorbic acid using AuNPs@polyaniline core–shell nanocomposites modified electrode. Talanta 89:136–141
48. Chen LC, Tseng KS, Ho KC (2006) General Kinetic Model for Amperometric Sensors Based on Prussian Blue Mediator and Its Analogs: Application to Cysteine Detection. Electroanalysis 18: 1313–1321
49. Elgrishi N, Rountree KJ, McCarthy BD, Rountree ES, Eisenhart TT, Dempsey JL (2018) A Practical Beginner's Guide to Cyclic Voltammetry. J Chem Educ 95:197–206
50. RahmanMM LJJ (2019) Electrochemical Dopamine Sensors Based on Graphene. J Electrochem Sci Technol 10(2):185–195
51. Maity D, Minitha CR, Kumar RTR (2019) Glucose oxidase immobilized amine terminated multiwall carbon nanotubes/reduced graphene oxide/polyaniline/gold nanoparticles modified screen-printed carbon electrode for highly sensitive amperometric glucose detection. Mater Sci Eng C Mater Biol Appl 105:110075
52. He W, Gui R, Jin H, Wang B, Bu X, Fu Y (2018) Ratiometric fluorescence and visual imaging detection of dopamine based on carbon dots/copper nanoclusters dual-emitting nanohybrids. Talanta 178:109–115
53. Zhao C, Jiao Y, Hua J, Yang J, Yang Y (2018) Hydrothermal Synthesis of Nitrogen-Doped Carbon Quantum Dots as Fluorescent Probes for the Detection of Dopamine. J Fluoresc 28(1):269–276
54. Li S, Ma Y, Liu Y, Xin G, Wang M, Zhang Z, Liu Z (2019) Electrochemical sensor based on a three dimensional nanostructured MoS2nanosphere-PANI/reduced graphene oxide composite for simultaneous detection of ascorbic acid, dopamine, and uric acid. RSC Adv 9(6):2997–3003
55. Algarra M, González-Calabuig A, Radotić K, Mutavdzic D, Ania CO, Lázaro-Martínez JM, Jiménez-Jiméneza J, Rodríguez-Castellón E, Del Valle M (2018) Enhanced electrochemical response of carbon quantum dot modified electrodes. Talanta 178: 679–685
56. Selvolini G, Lazzarini C, Marrazza G (2019) Electrochemical Nanocomposite Single-Use Sensor for Dopamine Detection. Sensors 19(14):3097
57. Prathap MA, Srivastava R (2013) Tailoring properties of polyaniline for simultaneous determination of a quaternary mixture of ascorbic acid, dopamine, uric acid, and tryptophan. Sensors Actuators B Chem 177:239–250

58. Bao Y, Song J, Mao Y, Han D, Yang F, Niu L, Ivaska A (2011) Graphene Oxide-Templated Polyaniline Microsheets toward Simultaneous Electrochemical Determination of AA/DA/UA. Electroanalysis 23(4):878–884
59. Demirkan B, Bozkurt S, Şavk A, Cellat K, Gülbağca F, Nas SN, Alma MH, Sen F (2019) Composites of Bimetallic Platinum-Cobalt Alloy Nanoparticles and Reduced Graphene Oxide for Electrochemical Determination of Ascorbic Acid, Dopamine, and Uric Acid. Sci Rep 9:12258